Acta Cryst E CRYSTALLOGRAPHIC COMMUNICATIONS

ISSN 2056-9890

Synthesis, structure and computational study of diacetatobis(2-amino-6-fluoro-1,3-benzothiazole-κN^3)zinc(II)

Dilshoda Amanova,[a] Zubaydabegim Radjabova,[b] Sardor Murodov,[b,c]* Sevinch Erkinboyeva,[b] Odil Choriev,[d] Jamshid Ashurov[d] and Shahlo Daminova[b,c]

[a]Termez Branch of Tashkent State Medical University, 64 Islom Karimov Street, Termiz 132000, Uzbekistan, [b]National University of Uzbekistan named after Mirzo Ulugbek, University Street, 4, Tashkent 100174, Uzbekistan, [c]Uzbekistan-Japan Innovation Centre of Youth, University Street 2B, Tashkent 100095, Uzbekistan, and [d]Institute of Bioorganic Chemistry, Academy of Sciences of Uzbekistan, Mirzo, Ulugbek Street 83, Tashkent 100125, Uzbekistan. *Correspondence e-mail: sardor.08122003@gmail.com

Received 20 August 2026
Accepted 1 September 2026

Edited by T. Akitsu, Tokyo University of Science, Japan

Keywords: crystal structure; 2-amino-6-fluoro-1,3-benzothiazole; Hirshfeld surface; Void analysis; π–π stacking.

CCDC reference: 2584886

Supporting information: this article has supporting information at journals.iucr.org/e

In the title zinc(II) complex, $[Zn(C_2H_3O_2)_2(C_7H_5FN_2S)_2]$, the Zn^{II} atom adopts a tetrahedral coordination geometry (τ_4 = 0.96), defined by two nitrogen atoms from two neutral 2-amino-6-fluoro-1,3-benzothiazole ligands and two oxygen atoms from two monodentately coordinated acetate anions. The crystal packing is governed by classical N—H···O hydrogen bonds, which generate one-dimensional chains extending along the [011] direction. These chains are further reinforced by bifurcated N—H···(O,F) hydrogen bonds together with C—H···π, O···π, and offset π–π interactions, resulting in a robust three-dimensional supramolecular framework. Hirshfeld surface analysis reveals that H···H (31.5%), C···H/H···C (16.3%), O···H/H···O (13.0%), F···H/H···F (12.9%), and S···H/H···S (10.2%) contacts make the largest contributions to the crystal packing, while a void analysis confirms the efficient packing of the molecules within the crystal.

1. Chemical context

Benzothiazole derivatives constitute an important class of nitrogen- and sulfur-containing heterocyclic compounds owing to their structural diversity, coordination versatility and broad spectrum of biological and physicochemical properties (Keri *et al.*, 2015). The presence of nitrogen and sulfur donor atoms within the fused aromatic framework provides favourable coordination sites for transition-metal ions, while substitution on the benzene ring enables systematic modulation of the electronic properties, molecular polarity and intermolecular interactions of the ligand. Consequently, substituted benzothiazoles have attracted considerable attention in coordination chemistry, crystal engineering and medicinal chemistry (Barbarossa *et al.*, 2023).

Particular interest has been devoted to 2-aminobenzothiazole derivatives because the heterocyclic nitrogen atom readily coordinates to metal centres, whereas the exocyclic amino group usually remains non-coordinated and serves as an efficient hydrogen-bond donor. This dual functionality facilitates the formation of coordination compounds together with extended supramolecular architectures sustained by classical and non-classical intermolecular interactions. Previous structural investigations have demonstrated that Zn^{II} complexes containing 2-aminobenzothiazole predominantly exhibit tetrahedral coordination environments in which the ligand binds through the ring nitrogen atom rather than the

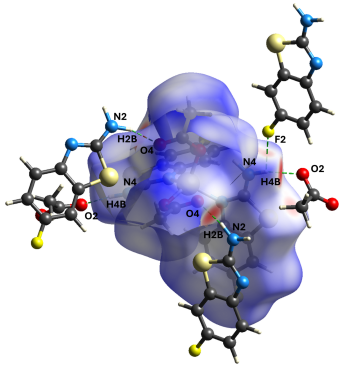

amino N atom (Davarski *et al.*, 1996; Kim & Kang, 2012; Suh *et al.*, 2009).

Fluorinated benzothiazole derivatives are considered particularly promising because fluorine substitution modifies the electronic distribution of the aromatic system without introducing significant steric effects. The strong electron-withdrawing character of fluorine influences the donor ability of the coordinating nitrogen atom and frequently contributes to crystal stabilization through weak intermolecular contacts, including N—H···F and C—H···F interactions. In addition, fluorination affects the π-electron density of the aromatic framework, thereby influencing aromatic stacking and other non-covalent interactions responsible for crystal packing (Li *et al.*, 2013; Kumar *et al.*, 2017).

The molecular structure of free 2-amino-6-fluoro-1,3-benzothiazole has previously shown that fluorine substitution preserves the near-planarity of the benzothiazole skeleton while allowing the formation of an extensive hydrogen-bonding network in the crystal. Such structural characteristics indicate that this ligand is well suited for the construction of coordination compounds in which both coordination and supramolecular interactions contribute to the overall crystal architecture (Jai-nhuknan *et al.*, 1997*a*,*b*).

Mixed-ligand Zn^{II} complexes containing nitrogen-donor heterocycles and carboxylate ligands have been widely investigated because of their structural diversity and their ability to generate robust supramolecular assemblies through hydrogen bonding and aromatic interactions. In many cases, acetate anions coordinate in a monodentate manner, leaving the second oxygen atom available for intermolecular hydrogen bonding, which plays an essential role in directing crystal packing (Guo *et al.*, 2011). Moreover, benzothiazole-based Zn^{II} complexes have attracted increasing attention owing to their potential biological activity and favourable structural characteristics arising from the combination of rigid aromatic ligands and flexible coordination environments (Babu *et al.*, 2015; Reddy *et al.*, 2014).

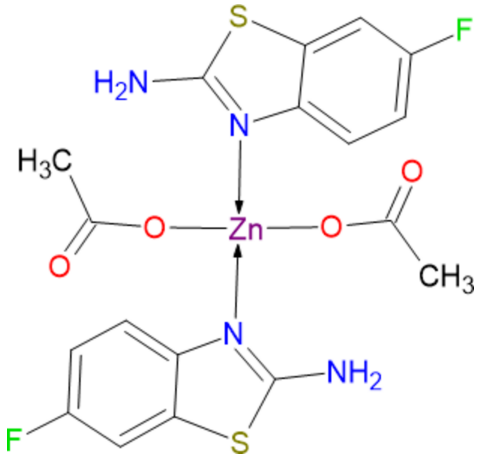

Motivated by these considerations, 2-amino-6-fluoro-1,3-benzothiazole was selected as a ligand combining a rigid aromatic framework, a strong nitrogen donor atom, an amino group capable of forming intermolecular hydrogen bonds and a fluorine substituent expected to influence crystal packing. Zinc acetate was employed as the metal precursor because acetate ions readily adopt monodentate coordination while simultaneously providing additional hydrogen-bond acceptor sites. As part of our continuing studies on coordination compounds of substituted benzothiazoles, the title compound, $[Zn(C_2H_3O_2)_2(C_7H_5FN_2S)_2]$, (I), was synthesized and its crystal structure, supramolecular organization, Hirshfeld surface and crystal void distribution were investigated.

Table 1
Selected geometric parameters (Å, °).

Zn1—O1	1.977 (3)	O1—C15	1.272 (5)
Zn1—O3	1.954 (2)	O3—C17	1.270 (4)
Zn1—N1	2.038 (3)	O4—C17	1.224 (5)
Zn1—N3	2.045 (3)	O2—C15	1.262 (5)
O3—Zn1—O1	119.78 (12)	N3—Zn1—O1	112.87 (11)
N1—Zn1—O1	104.15 (12)	N3—Zn1—O3	102.93 (10)
N1—Zn1—O3	109.13 (11)	N3—Zn1—N1	107.53 (11)

2. Structural commentary

The asymmetric unit of (I) comprises one independent neutral complex molecule (Fig. 1). The title compound crystallizes in the non-centrosymmetric Sohncke space group $Pna2_1$. The refined Flack parameter of 0.002 (12) confirms that the absolute structure has been reliably established. The Zn^{II} centre is coordinated by two nitrogen atoms from two 2-amino-6-fluoro-1,3-benzothiazole (AFBT) ligands and two oxygen atoms from two acetate (ac) anions, giving a four-coordinate ZnN_2O_2 environment.

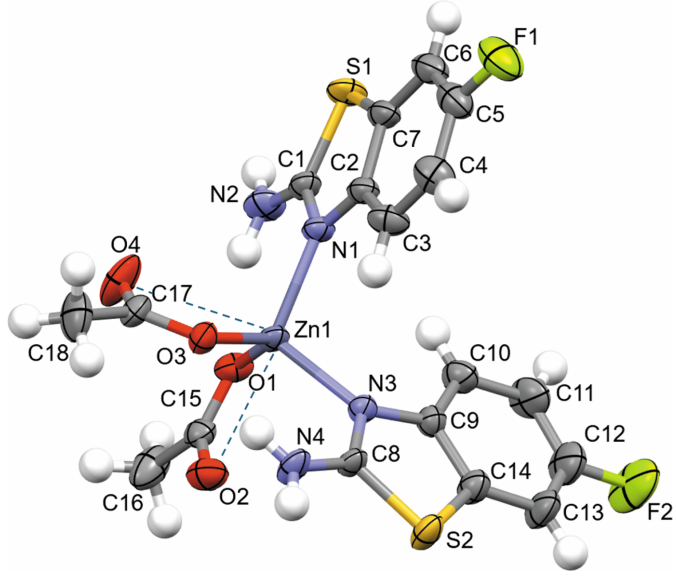

Figure 1
Molecular structure of the title compound, showing the atom-numbering scheme. Displacement ellipsoids are drawn at the 40% probability level.

The AFBT ligands coordinate exclusively through the endocyclic nitrogen atoms of the thiazole rings, whereas both ac anions adopt a monodentate coordination mode. The Zn—O and Zn—N bond lengths (Table 1) are consistent with those reported for structurally related Zn^{II} complexes containing 2-aminobenzothiazole derivatives, in which the Zn—N and Zn—O bond distances generally fall within the ranges 2.02–2.05 and 1.94–1.98 Å, respectively (Tojiboyeva *et al.*, 2025; Kim & Kang, 2012; Kim *et al.*, 2009).

The coordination geometry around the Zn^{II} centre is best described as a slightly distorted tetrahedron. Quantitative evaluation using the four-coordinate geometry index τ_4 proposed by Yang *et al.*, 2007, defined as $\tau_4 = [360 - (\alpha + \beta)]/141$, where α and β are the two largest coordination angles, gives a value of 0.96, indicating a tetrahedral geometry. The slight distortion from the ideal tetrahedron arises from the different donor characteristics of the nitrogen and oxygen atoms together with the spatial arrangement of the AFBT and ac ligands.

Although the *ac* anions coordinate in a monodentate fashion, short secondary contacts of Zn1···O2 = 2.674 (3) Å and Zn1···O4 = 2.819 (4) Å are observed. These separations are significantly longer than normal Zn—O coordination bonds and therefore cannot be regarded as additional coordination interactions. Nevertheless, they indicate the presence of weak secondary intramolecular Zn···O contacts, reflecting the spatial organization of the coordination environment.

Both AFBT ligands remain essentially planar after coordination. The root-mean-square (r.m.s.) deviations from the least-squares planes are 0.019 and 0.020 Å, confirming that the π-conjugated benzothiazole framework is well preserved upon coordination. Furthermore, the geometry of the coordinated ligands closely resembles that of the free AFBT molecule, indicating that coordination to the Zn^{II} centre has little influence on the molecular structure of the heterocyclic fragment (Jai-nhuknan *et al.*, 1997*a*,*b*).

The ac groups exhibit the characteristic asymmetry of the C—O bond lengths expected for monodentate carboxylate ligands. Coordination occurs through only one oxygen atom of each ac anion, while the second oxygen atom remains uncoordinated, resulting in the observed differentiation of the C—O bond lengths.

3. Supramolecular features

The crystal packing is governed by a combination of classical hydrogen bonds and weaker non-covalent interactions, which collectively generate a robust three-dimensional supramolecular architecture (Fig. 2). The principal contribution to the crystal packing arises from classical N—H···O hydrogen bonds formed between the amino groups of the AFBT ligands and the non-coordinating oxygen atoms of the ac anions (Table 2). In particular, the N2—H2*B*···O4 and N4—H4*B*···O2 hydrogen bonds link adjacent molecules into infinite chains propagating along the [011] direction.

Besides forming classical hydrogen bonds, atom N4 also participates in a bifurcated hydrogen bond, where hydrogen atom H4*B* simultaneously interacts with atoms O2 and F2. The N4—H4*B*···F2 contact is considerably weaker than the corresponding N—H···O hydrogen bond; however, it plays an important structure-directing role. Although fluorine is generally regarded as a weak hydrogen-bond acceptor, the N—H···F interaction links adjacent hydrogen-bonded chains and reinforces the overall supramolecular framework. Thus, the fluorine substituents do not constitute the primary packing motif but act as secondary acceptors that enhance the connectivity and stability of the crystal structure.

The crystal packing is further reinforced by weak C—H···π and O···π interactions. The methyl group of the ac ligand forms a C18—H18*B*···*Cg*6 contact, where *Cg*6 is the centroid of the benzothiazole ring system (S1/C1/N1/C2/C3/C4/C5/C6/C7). The corresponding geometric parameters are H18*B*···*Cg*6 = 2.972 (19) Å, C18···*Cg*6 = 3.565 (5) Å and C18—H18*B*···*Cg*6 = 121.1 (13)°, which are typical of weak but significant C—H···π interactions. In addition, the carbonyl oxygen atom O4 is involved in an O···π interaction

Table 2
Hydrogen-bond geometry (Å, °).

*Cg*1 and *Cg*6 are the centroids of the Zn1/O1/C15/O2 and S1/N1/C1–C7 rings, respectively.

D—H···*A*	*D*—H	H···*A*	*D*···*A*	*D*—H···*A*
N2—H2B···O4^{i}	0.86 (1)	1.97 (1)	2.806 (5)	162 (1)
N4—H4B···F2^{ii}	0.86 (1)	2.44 (1)	2.910 (6)	115 (1)
N4—H4B···O2^{iii}	0.86 (1)	2.07 (1)	2.890 (4)	160 (1)
C18—H18B···*Cg*6^{iv}	0.96 (2)	2.97 (2)	3.565 (5)	121 (1)
C17—O4···*Cg*1	1.22 (1)	3.08 (1)	3.234 (4)	86 (1)

Symmetry codes: (i) $-x+1, -y+1, z+\frac{1}{2}$; (ii) $x+\frac{1}{2}, -y+\frac{3}{2}, z-1$; (iii) $x+\frac{1}{2}, -y+\frac{3}{2}, z$; (iv) $x, y, z-1$.

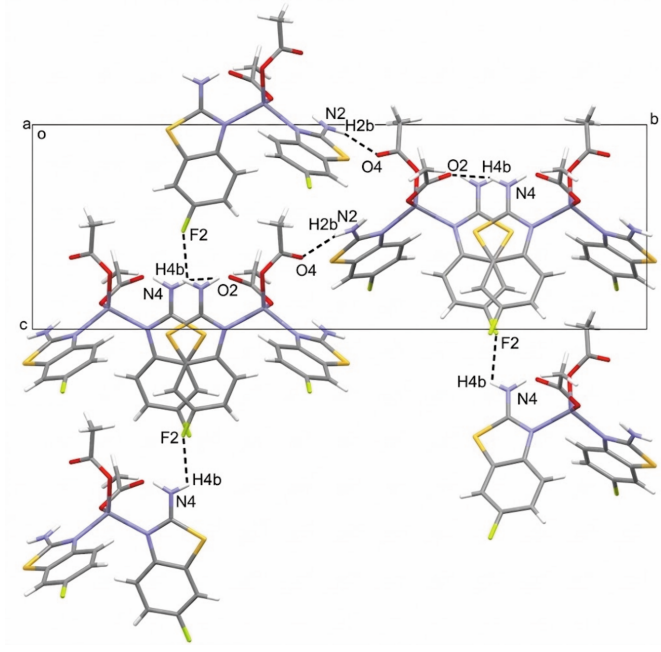

Figure 2
Crystal packing of the title compound viewed along the [011] direction, showing the network of N—H···O and N—H···F hydrogen bonds. Hydrogen bonds are shown as dashed lines.

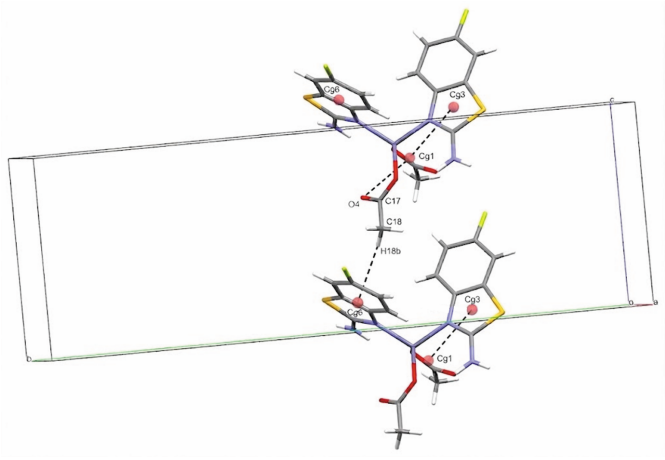

Figure 3
View of the π-related intermolecular interactions in the crystal structure of the title compound, showing the offset π–π stacking interaction ($Cg1\cdots Cg3$), the C18—H18$B\cdots Cg6$ C—H$\cdots\pi$ interaction, and the C17—O4$\cdots Cg1$ O$\cdots\pi$ contact. Selected interactions are shown as dashed lines.

with the centroid $Cg1$ of the coordination plane (Zn1/O1/C15/O2), with an O4$\cdots Cg1$ separation of 3.075 (4) Å (Fig. 3). Although individually weak, these contacts complement the hydrogen-bonding network and contribute to the efficient packing of the molecules within the crystal.

A further characteristic feature of the crystal structure is the presence of a π–π interaction between centroids $Cg1$ and $Cg3$, where $Cg3$ corresponds to the thiazole ring (S2/C8/N3/C9/C14). The centroid-to-centroid distance of 3.7559 (19) Å falls within the range typically associated with offset π–π stacking interactions. This arrangement promotes favourable overlap of the π-electron systems while minimizing steric repulsion, thereby providing additional stabilization to the crystal packing.

4. Hirshfeld surface

To obtain a deeper insight into the intermolecular interactions governing the crystal packing, a Hirshfeld surface analysis was carried out using *CrystalExplorer21.5* (Spackman *et al.*, 2021). The Hirshfeld surface mapped over d_{norm} is shown in Fig. 4. The Hirshfeld surface has a total area of 444.97 Å^2 and an enclosed volume of 517.52 Å^3. The most intense red regions on the d_{norm} surface are localized around the non-coordinating oxygen atoms of the *ac* ligands and the amino groups of the benzothiazole molecules, corresponding to the shortest intermolecular N—H$\cdots$O hydrogen bonds identified in the crystal structure. Less pronounced red spots are observed around the fluorine atoms, confirming their involvement in weaker N—H$\cdots$F interactions that complement the classical hydrogen-bonding network.

The two-dimensional fingerprint plots reveal that H$\cdots$H contacts make the largest contribution to the Hirshfeld surface, accounting for 31.5% of the total surface area (Fig. 5). This predominance is characteristic of hydrogen-rich molecular crystals and mainly reflects the close packing of

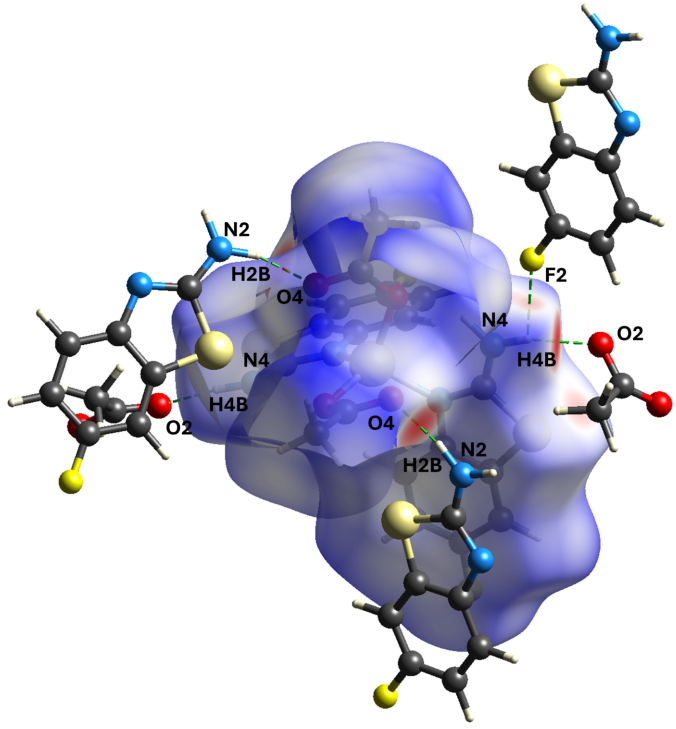

Figure 4
Hirshfeld surface of the title compound mapped over d_{norm}, showing the intermolecular contacts responsible for the crystal packing.

neighbouring molecules. The second-largest contribution arises from C$\cdots$H/H$\cdots$C contacts (16.3%), which are associated primarily with the C—H$\cdots\pi$ interactions between the acetate methyl groups and the aromatic benzothiazole fragments. Although individually weak, these interactions contribute significantly to the stabilization of the crystal packing.

The O$\cdots$H/H$\cdots$O contacts contribute 13.0% to the Hirshfeld surface and are directly associated with the classical N—H$\cdots$O hydrogen bonds forming the principal supramolecular framework. Their characteristic sharp spikes on the

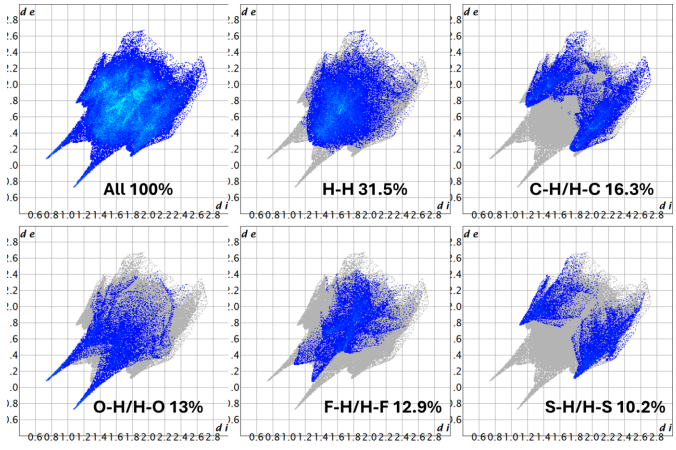

Figure 5
Two-dimensional fingerprint plots of the title compound showing the overall contacts and the individual contributions of H$\cdots$H, C$\cdots$H/H$\cdots$C, O$\cdots$H/H$\cdots$O, F$\cdots$H/H$\cdots$F and S$\cdots$H/H$\cdots$S interactions to the Hirshfeld surface.

fingerprint plots indicate the presence of strong directional hydrogen bonds. A comparable contribution is observed for F···H/H···F contacts (12.9%), demonstrating that the fluorine substituents participate actively in the intermolecular interaction network. Although fluorine is generally considered a weak hydrogen-bond acceptor, its involvement in the bifurcated N—H···(O,F) hydrogen bond highlights its important auxiliary role in reinforcing the hydrogen-bonded framework generated by the stronger N—H···O interactions.

The contribution of S···H/H···S contacts reaches 10.2%, reflecting numerous van der Waals contacts involving the sulfur atoms of the benzothiazole rings. The remaining interactions make considerably smaller contributions, including S···C/C···S (3.5%), C···C (2.6%), C···F/F···C (2.5%), O···S/S···O (1.9%), F···N/N···F (1.5%), F···O/O···F (1.3%), N···H/H···N and F···S/S···F (each 1.0%), N···S/S···N (0.6%), and C···N/N···C, C···O/O···C, and F···F (each 0.1%). Although individually insignificant, these weak contacts collectively contribute to the overall stabilization of the crystal packing.

5. Database survey

A search of the Cambridge Structural Database (CSD, Version 2026.2.0; Groom *et al.*, 2016) revealed only three structurally related transition-metal complexes containing benzothiazole-based ligands. Two entries, NOGZUG and NOHBAP (Sahoo *et al.*, 2014), are Cu^{II} complexes featuring cyclometallated imidazolidine–benzothiazole ligands, while QAYKOU (Akhter *et al.*, 2022) is a Ru^{II} η^6-*p*-cymene complex containing an aminobenzothiazole derivative. All of these structures differ significantly from the title compound in both coordination mode and metal coordination geometry. To the best of our knowledge, no closely related Zn^{II} complex containing two neutral AFBT ligands together with two monodentately coordinated acetate anions has previously been reported.

6. Synthesis and crystallization

The following solutions were prepared: (*a*) an ethanolic solution of a $Zn(CH_3COO)_2{\cdot}4H_2O$ (1.0 mmol) and (*b*) an ethanolic solution of AFBT (2.0 mmol). Solution (*a*) was added to solution (*b*), and the resulting mixture was stirred at room temperature for 12 h using magnetic stirring. A crystalline precipitate was formed, filtered off, washed several times with ethanol and dried in air. Since the obtained material was readily soluble in dimethylformamide (DMF), it was recrystallized from this solvent. No poor solvent was used to induce crystallization; instead, the product precipitated directly from the ethanolic reaction mixture because of its limited solubility in ethanol, yielding well-formed whitish single crystals suitable for X-ray diffraction analysis and further physicochemical investigations. The reaction scheme is shown in Fig. 6.

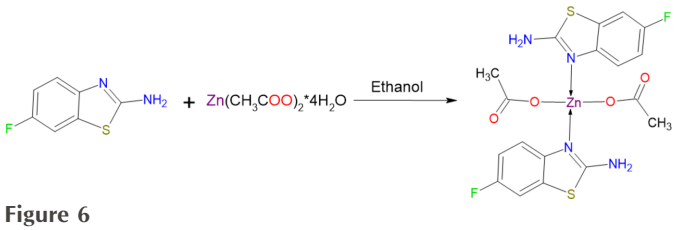

Figure 6
Reaction scheme.

Table 3
Experimental details.

Crystal data	
Chemical formula	$[Zn(C_2H_3O_2)_2(C_7H_5FN_2S)_2]$
M_r	519.88
Crystal system, space group	Orthorhombic, $Pna2_1$
Temperature (K)	273
a, *b*, *c* (Å)	8.26379 (13), 27.6342 (3), 9.21400 (12)
V (Å^3)	2104.14 (5)
Z	4
Radiation type	Cu $K\alpha$
μ (mm^{-1})	3.95
Crystal size (mm)	0.37 × 0.28 × 0.25
Data collection	
Diffractometer	XtaLAB Synergy, Single source at home/near, HyPix3000
Absorption correction	Multi-scan (*CrysAlis PRO*; Rigaku OD, 2023)
T_{min}, T_{max}	0.336, 1.000
No. of measured, independent and observed [$I \geq 2\sigma(I)$] reflections	19982, 4036, 3829
R_{int}	0.063
(sin $\theta/\lambda)_{max}$ (Å^{-1})	0.616
Refinement	
$R[F^2 > 2\sigma(F^2)]$, $wR(F^2)$, S	0.040, 0.113, 1.03
No. of reflections	4036
No. of parameters	282
No. of restraints	1
H-atom treatment	H-atom parameters constrained
$\Delta\rho_{max}$, $\Delta\rho_{min}$ (e Å^{-3})	0.38, −0.60
Absolute structure	Hooft et al. (2010)
Absolute structure parameter	0.002 (12)

Computer programs: *CrysAlis PRO* (Rigaku OD, 2023), *SHELXT* (Sheldrick, 2015), *OLEX2.refine* (Bourhis *et al.*, 2015) and *OLEX2* (Dolomanov *et al.*, 2009).

7. Refinement

Crystal data, data collection and structure refinement details are summarized in Table 3. All non-hydrogen atoms were refined anisotropically. Hydrogen atoms bonded to carbon atoms were positioned geometrically and refined using a riding model with C—H = 0.93–0.96 Å and U_{iso}(H) = 1.2U_{eq}(C) for aromatic carbon atoms and 1.5U_{eq}(C) for methyl groups. Hydrogen atoms attached to nitrogen atoms were located from difference-Fourier maps and refined with restrained N—H distances of 0.86 Å, with U_{iso}(H) = 1.2U_{eq}(N).

Acknowledgements

The authors thank the Institute of Bioorganic Chemistry of the Academy of Sciences of Uzbekistan for providing access

to the XtaLAB Synergy-S X-ray diffractometer. They also acknowledge the Uzbek-Japan Innovation Center of Youth for providing access to the analytical instrumentation and research facilities used in this work.

References

Akhter, S., Rehman, A., Abidi, S. M. A., Arjmand, F. & Tabassum, S. (2022). *New J. Chem.* **46**, 11462–11473.

Babu, H. S., Suresh, T. & Kotresh, D. (2015). *Int. J. Pharm. Life Sci.* **6**, 4708–4714.

Barbarossa, A., Ceramella, J., Carocci, A., Iacopetta, D., Rosato, A., Limongelli, F., Sicoli, G., *et al.* (2023). *Antibiotics* **12**, 1651.

Bourhis, L. J., Dolomanov, O. V., Gildea, R. J., Howard, J. A. K. & Puschmann, H. (2015). *Acta Cryst.* A**71**, 59–75.

Davarski, B., Jordanov, J., Mitewa, M. & Stanoeva, E. (1996). *Synth. React. Inorg. Met.-Org. Chem.* **26**, 757–765.

Dolomanov, O. V., Bourhis, L. J., Gildea, R. J., Howard, J. A. K. & Puschmann, H. (2009). *J. Appl. Cryst.* **42**, 339–341.

Groom, C. R., Bruno, I. J., Lightfoot, M. P. & Ward, S. C. (2016). *Acta Cryst.* B**72**, 171–179.

Guo, H., Zhang, Y., Liu, J. & Wang, X. (2011). *Asian J. Chem.* **23**, 3937–3940.

Hooft, R. W. W., Straver, L. H. & Spek, A. L. (2010). *J. Appl. Cryst.* **43**, 665–668.

Jai-nhuknan, J., Karipides, A. G., Hughes, J. M. & Cantrell, J. S. (1997*a*). *Acta Cryst.* C**53**, 381–383.

Jai-nhuknan, J., Karipides, A. G., Hughes, J. M. & Cantrell, J. S. (1997*b*). *Acta Cryst.* C**53**, 381–383.

Keri, R. S., Patil, M. R., Patil, S. A. & Budagumpi, S. (2015). *Eur. J. Med. Chem.* **89**, 207–251.

Kim, Y.-I. & Kang, S. K. (2012). *Acta Cryst.* E**68**, m178–m179.

Kim, N.-H., Hwang, I.-C. & Ha, K. (2009). *Acta Cryst.* E**65**, m667.

Kumar, S., Basappa Chidananda, V. K., Hosakere Doddarevanna, R., Hamse Kameshwar, V., Kaur, M. & Jasinski, J. P. (2017). *J. Mol. Struct.* **1142**, 293–303.

Li, X., Wang, Y., Liu, Y., Zhang, H., *et al.* (2013). *Inorg. Chem.* **52**, 2063–2072.

Reddy, D. R. S., Jamullamudi, R. N., Pedamallu, N. & Rani, A. P. (2014). *Int. J. Pharm. Sci. Rev. Res.* **28**, 189–194.

Rigaku OD (2023). *CrysAlis PRO*. Rigaku Oxford Diffraction, Yarnton, England.

Sahoo, S. K., Jena, H. S., Majji, G. & Patel, B. K. (2014). *Synthesis* **46**, 1886–1900.

Sheldrick, G. M. (2015). *Acta Cryst.* A**71**, 3–8.

Spackman, P. R., Turner, M. J., McKinnon, J. J., Wolff, S. K., Grimwood, D. J., Jayatilaka, D. & Spackman, M. A. (2021). *J. Appl. Cryst.* **54**, 1006–1011.

Tojiboyeva, I., Murodov, S., Makhmudova, L., Ziyatov, D., Ashurov, J. & Daminova, S. (2025). *Acta Cryst.* E**81**, 948–953.

Yang, L., Powell, D. R. & Houser, R. P. (2007). *Dalton Trans.* pp. 955–964.

supporting information

Acta Cryst. (2026). E**82** [https://doi.org/10.1107/S2056989026009163]

Synthesis, structure and computational study of diacetatobis(2-amino-6-fluoro-1,3-benzothiazole-κN^3)zinc(II)

Dilshoda Amanova, Zubaydabegim Radjabova, Sardor Murodov, Sevinch Erkinboyeva, Odil Choriev, Jamshid Ashurov and Shahlo Daminova

Computing details

Diacetatobis(2-amino-6-fluoro-1,3-benzothiazole-κN^3)zinc(II)

Crystal data

$[Zn(C_2H_3O_2)_2(C_7H_5FN_2S)_2]$
M_r = 519.88
Orthorhombic, $Pna2_1$
a = 8.26379 (13) Å
b = 27.6342 (3) Å
c = 9.21400 (12) Å
V = 2104.14 (5) Å^3
Z = 4
$F(000)$ = 1055.915
D_x = 1.641 Mg m^{-3}
Cu $K\alpha$ radiation, λ = 1.54184 Å
Cell parameters from 4970 reflections
θ = 3.7–71.1°
μ = 3.95 mm^{-1}
T = 273 K
Rhombohedral, clear whiteish colourless
0.37 × 0.28 × 0.25 mm

Data collection

XtaLAB Synergy, Single source at home/near, HyPix3000 diffractometer
ω scans
Absorption correction: multi-scan (CrysAlisPro; Rigaku OD, 2023)
T_{min} = 0.336, T_{max} = 1.000
19982 measured reflections
4036 independent reflections
3829 reflections with $I \geq 2\sigma(I)$
R_{int} = 0.063
θ_{max} = 71.7°, θ_{min} = 3.2°
h = −10→10
k = −33→26
l = −11→11

Refinement

Refinement on F^2
Least-squares matrix: full
$R[F^2 > 2\sigma(F^2)]$ = 0.040
$wR(F^2)$ = 0.113
S = 1.03
4036 reflections
282 parameters
1 restraint
26 constraints
Primary atom site location: dual
H-atom parameters constrained
$w = 1/[\sigma^2(F_o^2) + (0.0835P)^2]$ where $P = (F_o^2 + 2F_c^2)/3$
$(\Delta/\sigma)_{max}$ = 0.001
$\Delta\rho_{max}$ = 0.38 e Å^{-3}
$\Delta\rho_{min}$ = −0.59 e Å^{-3}
Absolute structure: Hooft et al. (2010)
Absolute structure parameter: 0.002 (12)

Special details

Refinement. The structure was solved by direct methods and refined by full-matrix least-squares on F^2.

Fractional atomic coordinates and isotropic or equivalent isotropic displacement parameters (Å²)

	x	*y*	*z*	U_{iso}*/U_{eq}
Zn1	0.63340 (5)	0.623334 (12)	0.39621 (5)	0.03898 (13)
S2	0.72351 (14)	0.77996 (3)	0.52443 (10)	0.0590 (3)
S1	0.72502 (15)	0.48713 (3)	0.66695 (11)	0.0644 (3)
O1	0.3990 (3)	0.61134 (9)	0.3732 (3)	0.0533 (6)
O3	0.7725 (3)	0.62617 (8)	0.2249 (3)	0.0451 (5)
N1	0.7101 (4)	0.56872 (9)	0.5279 (3)	0.0432 (6)
N3	0.6824 (3)	0.68720 (9)	0.4992 (3)	0.0392 (5)
F1	1.2953 (4)	0.54886 (14)	0.8032 (4)	0.0932 (9)
F2	0.4525 (8)	0.75495 (15)	1.0179 (4)	0.1439 (19)
O4	0.6401 (4)	0.56292 (12)	0.1497 (5)	0.0902 (13)
O2	0.4259 (4)	0.67805 (10)	0.2456 (3)	0.0654 (7)
N2	0.4771 (4)	0.52090 (11)	0.5138 (4)	0.0626 (9)
H2a	0.4271 (4)	0.54166 (11)	0.4607 (4)	0.0751 (11)*
H2b	0.4299 (4)	0.49437 (11)	0.5382 (4)	0.0751 (11)*
N4	0.8032 (4)	0.72560 (10)	0.2979 (4)	0.0555 (8)
H4a	0.8114 (4)	0.69899 (10)	0.2500 (4)	0.0667 (10)*
H4b	0.8368 (4)	0.75225 (10)	0.2603 (4)	0.0667 (10)*
C17	0.7393 (4)	0.59503 (13)	0.1281 (4)	0.0479 (8)
C8	0.7392 (4)	0.72552 (10)	0.4282 (4)	0.0419 (7)
C9	0.6236 (4)	0.69968 (13)	0.6361 (4)	0.0452 (7)
C2	0.8639 (4)	0.56674 (12)	0.5905 (4)	0.0472 (8)
C16	0.1759 (6)	0.6390 (2)	0.2183 (7)	0.0813 (16)
H16a	0.114 (2)	0.6150 (14)	0.269 (4)	0.122 (2)*
H16b	0.123 (3)	0.6698 (6)	0.226 (5)	0.122 (2)*
H16c	0.1849 (6)	0.6301 (19)	0.1179 (16)	0.122 (2)*
C15	0.3419 (4)	0.64213 (12)	0.2842 (4)	0.0474 (7)
C5	1.1534 (5)	0.5536 (2)	0.7335 (5)	0.0662 (11)
C14	0.6342 (5)	0.74928 (14)	0.6671 (5)	0.0546 (9)
C4	1.1284 (5)	0.5957 (2)	0.6536 (6)	0.0689 (12)
H4	1.2085 (5)	0.6192 (2)	0.6478 (6)	0.0827 (14)*
C3	0.9818 (5)	0.60183 (15)	0.5827 (5)	0.0595 (10)
H3	0.9630 (5)	0.62987 (15)	0.5295 (5)	0.0714 (11)*
C7	0.8947 (5)	0.52462 (13)	0.6702 (4)	0.0544 (9)
C11	0.5019 (7)	0.6876 (2)	0.8684 (5)	0.0823 (15)
H11	0.4590 (7)	0.6673 (2)	0.9391 (5)	0.0987 (18)*
C10	0.5564 (5)	0.66893 (14)	0.7380 (5)	0.0588 (9)
H10	0.5480 (5)	0.63597 (14)	0.7190 (5)	0.0705 (11)*
C1	0.6246 (4)	0.52965 (12)	0.5575 (4)	0.0463 (8)
C12	0.5122 (8)	0.7365 (2)	0.8919 (6)	0.0893 (16)
C6	1.0398 (6)	0.51766 (16)	0.7425 (5)	0.0659 (11)
H6	1.0594 (6)	0.48958 (16)	0.7953 (5)	0.0791 (14)*
C13	0.5779 (8)	0.76845 (16)	0.7965 (5)	0.0783 (14)
H13	0.5848 (8)	0.80134 (16)	0.8171 (5)	0.0940 (17)*
C18	0.8288 (7)	0.5981 (3)	−0.0116 (5)	0.0884 (17)
H18a	0.925 (3)	0.5785 (14)	−0.0062 (19)	0.133 (2)*

H18b	0.761 (2)	0.5866 (17)	−0.0889 (9)	0.133 (2)*
H18c	0.859 (5)	0.6311 (4)	−0.030 (3)	0.133 (2)*

Atomic displacement parameters (Å²)

	U^{11}	U^{22}	U^{33}	U^{12}	U^{13}	U^{23}
Zn1	0.0520 (2)	0.02471 (19)	0.0402 (2)	−0.00300 (13)	0.0056 (2)	0.00357 (17)
S2	0.0945 (7)	0.0323 (4)	0.0502 (5)	−0.0112 (4)	0.0182 (5)	−0.0093 (3)
S1	0.0973 (7)	0.0342 (4)	0.0616 (5)	0.0019 (4)	0.0018 (6)	0.0195 (4)
O1	0.0536 (12)	0.0375 (11)	0.0689 (19)	0.0022 (9)	0.0021 (13)	0.0025 (12)
O3	0.0573 (13)	0.0375 (12)	0.0404 (12)	−0.0056 (9)	0.0056 (10)	−0.0060 (9)
N1	0.0580 (16)	0.0279 (12)	0.0437 (14)	0.0009 (11)	0.0044 (12)	0.0064 (11)
N3	0.0520 (14)	0.0313 (11)	0.0343 (12)	−0.0046 (10)	0.0064 (11)	0.0016 (10)
F1	0.0766 (17)	0.121 (3)	0.0819 (19)	0.0238 (17)	−0.0143 (16)	0.020 (2)
F2	0.257 (5)	0.100 (3)	0.075 (2)	0.020 (3)	0.092 (3)	−0.0093 (19)
O4	0.104 (3)	0.0625 (19)	0.104 (3)	−0.0374 (18)	0.022 (2)	−0.043 (2)
O2	0.0765 (18)	0.0472 (14)	0.0725 (19)	0.0039 (13)	0.0058 (17)	0.0103 (13)
N2	0.078 (2)	0.0347 (13)	0.075 (2)	−0.0137 (14)	−0.0018 (19)	0.0155 (15)
N4	0.091 (2)	0.0297 (12)	0.0464 (16)	−0.0151 (14)	0.0216 (17)	−0.0044 (12)
C17	0.0562 (19)	0.0389 (16)	0.0485 (18)	0.0035 (13)	0.0039 (15)	−0.0134 (14)
C8	0.0596 (18)	0.0242 (13)	0.0418 (18)	−0.0048 (11)	0.0059 (13)	−0.0026 (11)
C9	0.059 (2)	0.0412 (16)	0.0354 (16)	0.0011 (13)	0.0044 (14)	−0.0006 (13)
C2	0.068 (2)	0.0344 (16)	0.0388 (17)	0.0100 (13)	0.0079 (14)	0.0065 (13)
C16	0.056 (2)	0.081 (3)	0.108 (4)	0.006 (2)	−0.011 (3)	−0.039 (3)
C15	0.0567 (18)	0.0388 (17)	0.0466 (18)	0.0095 (14)	0.0070 (15)	−0.0027 (15)
C5	0.064 (2)	0.084 (3)	0.050 (2)	0.018 (2)	−0.0005 (19)	0.012 (2)
C14	0.074 (3)	0.0451 (19)	0.044 (2)	−0.0015 (16)	0.0128 (17)	−0.0036 (16)
C4	0.059 (2)	0.079 (3)	0.069 (3)	−0.0004 (19)	0.005 (2)	0.015 (3)
C3	0.063 (2)	0.0509 (19)	0.065 (2)	0.0026 (16)	0.0052 (18)	0.0197 (18)
C7	0.084 (2)	0.0404 (17)	0.0386 (18)	0.0153 (16)	0.0086 (17)	0.0085 (15)
C11	0.118 (4)	0.078 (3)	0.051 (3)	0.007 (3)	0.032 (3)	0.018 (2)
C10	0.076 (3)	0.0508 (19)	0.0498 (19)	0.0034 (18)	0.0124 (19)	0.0103 (16)
C1	0.068 (2)	0.0300 (15)	0.0408 (17)	−0.0015 (13)	0.0076 (15)	0.0037 (13)
C12	0.136 (5)	0.081 (3)	0.051 (2)	0.017 (3)	0.029 (3)	−0.011 (3)
C6	0.086 (3)	0.062 (2)	0.049 (2)	0.027 (2)	0.005 (2)	0.0136 (18)
C13	0.132 (4)	0.054 (2)	0.049 (2)	0.008 (3)	0.026 (3)	−0.0112 (19)
C18	0.101 (4)	0.116 (5)	0.048 (2)	0.002 (4)	0.013 (3)	−0.025 (3)

Geometric parameters (Å, º)

Zn1—O1	1.977 (3)	C9—C14	1.403 (5)
Zn1—O3	1.954 (2)	C9—C10	1.383 (5)
Zn1—N1	2.038 (3)	C2—C3	1.377 (5)
Zn1—N3	2.045 (3)	C2—C7	1.399 (5)
S2—C8	1.751 (3)	C16—H16a	0.9600
S2—C14	1.729 (4)	C16—H16b	0.9600
S1—C7	1.744 (4)	C16—H16c	0.9600
S1—C1	1.757 (4)	C16—C15	1.503 (6)

O1—C15	1.272 (5)	C5—C4	1.392 (7)
O3—C17	1.270 (4)	C5—C6	1.369 (7)
N1—C2	1.397 (5)	C14—C13	1.386 (6)
N1—C1	1.319 (4)	C4—H4	0.9300
N3—C8	1.330 (4)	C4—C3	1.387 (6)
N3—C9	1.395 (4)	C3—H3	0.9300
F1—C5	1.343 (5)	C7—C6	1.386 (6)
F2—C12	1.361 (6)	C11—H11	0.9300
O4—C17	1.224 (5)	C11—C10	1.383 (6)
O2—C15	1.262 (5)	C11—C12	1.371 (8)
N2—H2a	0.8600	C10—H10	0.9300
N2—H2b	0.8600	C12—C13	1.358 (8)
N2—C1	1.306 (5)	C6—H6	0.9300
N4—H4a	0.8600	C13—H13	0.9300
N4—H4b	0.8600	C18—H18a	0.9600
N4—C8	1.312 (5)	C18—H18b	0.9600
C17—C18	1.487 (6)	C18—H18c	0.9600
Cg1···Cg3	3.7559 (19)		
O3—Zn1—O1	119.78 (12)	C16—C15—O1	124.1 (4)
N1—Zn1—O1	104.15 (12)	C16—C15—O2	115.7 (4)
N1—Zn1—O3	109.13 (11)	C4—C5—F1	117.6 (5)
N3—Zn1—O1	112.87 (11)	C6—C5—F1	119.9 (4)
N3—Zn1—O3	102.93 (10)	C6—C5—C4	122.4 (4)
N3—Zn1—N1	107.53 (11)	C9—C14—S2	110.5 (3)
C14—S2—C8	89.73 (17)	C13—C14—S2	127.6 (3)
C1—S1—C7	89.56 (17)	C13—C14—C9	121.9 (4)
C15—O1—Zn1	108.7 (2)	H4—C4—C5	120.6 (3)
C17—O3—Zn1	114.4 (2)	C3—C4—C5	118.8 (4)
C2—N1—Zn1	123.9 (2)	C3—C4—H4	120.6 (3)
C1—N1—Zn1	124.3 (2)	C4—C3—C2	120.5 (4)
C1—N1—C2	111.7 (3)	H3—C3—C2	119.8 (2)
C8—N3—Zn1	121.9 (2)	H3—C3—C4	119.8 (3)
C9—N3—Zn1	124.3 (2)	C2—C7—S1	109.8 (3)
C9—N3—C8	111.8 (3)	C6—C7—S1	128.4 (3)
H2b—N2—H2a	120.0	C6—C7—C2	121.7 (4)
C1—N2—H2a	120.0	C10—C11—H11	120.5 (3)
C1—N2—H2b	120.0	C12—C11—H11	120.5 (3)
H4b—N4—H4a	120.0	C12—C11—C10	119.0 (4)
C8—N4—H4a	120.0	C11—C10—C9	119.4 (4)
C8—N4—H4b	120.0	H10—C10—C9	120.3 (2)
O4—C17—O3	121.5 (4)	H10—C10—C11	120.3 (3)
C18—C17—O3	117.5 (4)	N1—C1—S1	114.4 (3)
C18—C17—O4	121.0 (4)	N2—C1—S1	119.6 (3)
N3—C8—S2	114.1 (2)	N2—C1—N1	126.0 (3)
N4—C8—S2	119.5 (2)	C11—C12—F2	118.8 (5)
N4—C8—N3	126.4 (3)	C13—C12—F2	117.0 (5)

C14—C9—N3	113.8 (3)	C13—C12—C11	124.3 (4)
C10—C9—N3	127.0 (3)	C7—C6—C5	117.6 (4)
C10—C9—C14	119.2 (3)	H6—C6—C5	121.2 (2)
C3—C2—N1	126.5 (3)	H6—C6—C7	121.2 (2)
C7—C2—N1	114.5 (3)	C12—C13—C14	116.3 (4)
C7—C2—C3	119.0 (4)	H13—C13—C14	121.9 (3)
H16b—C16—H16a	109.5	H13—C13—C12	121.9 (3)
H16c—C16—H16a	109.5	H18a—C18—C17	109.5
H16c—C16—H16b	109.5	H18b—C18—C17	109.5
C15—C16—H16a	109.5	H18b—C18—H18a	109.5
C15—C16—H16b	109.5	H18c—C18—C17	109.5
C15—C16—H16c	109.5	H18c—C18—H18a	109.5
O2—C15—O1	120.2 (4)	H18c—C18—H18b	109.5

Zn1—O1—C15—O2	−11.6 (3)	F1—C5—C6—C7	179.2 (4)
Zn1—O1—C15—C16	168.2 (3)	F2—C12—C11—C10	177.4 (6)
Zn1—O3—C17—O4	−7.8 (3)	F2—C12—C13—C14	−178.3 (6)
Zn1—O3—C17—C18	174.0 (3)	N2—C1—S1—C7	179.5 (3)
Zn1—N1—C2—C3	4.9 (4)	N2—C1—N1—C2	−179.7 (4)
Zn1—N1—C2—C7	−176.3 (3)	N4—C8—S2—C14	179.6 (4)
Zn1—N1—C1—S1	176.9 (2)	N4—C8—N3—C9	179.6 (4)
Zn1—N1—C1—N2	−3.4 (3)	C8—S2—C14—C9	1.1 (2)
Zn1—N3—C8—S2	164.4 (2)	C8—S2—C14—C13	−178.8 (4)
Zn1—N3—C8—N4	−15.8 (3)	C8—N3—C9—C14	1.1 (3)
Zn1—N3—C9—C14	−163.0 (3)	C8—N3—C9—C10	−180.0 (3)
Zn1—N3—C9—C10	15.9 (4)	C9—C14—C13—C12	0.1 (5)
S2—C8—N3—C9	−0.2 (3)	C9—C10—C11—C12	1.6 (6)
S2—C14—C9—N3	−1.5 (3)	C2—C3—C4—C5	−0.5 (5)
S2—C14—C9—C10	179.5 (3)	C2—C7—S1—C1	0.7 (3)
S2—C14—C13—C12	180.0 (6)	C2—C7—C6—C5	0.0 (4)
S1—C7—C2—N1	−0.5 (3)	C14—C9—C10—C11	−0.3 (5)
S1—C7—C2—C3	178.4 (3)	C14—C13—C12—C11	1.3 (8)
S1—C7—C6—C5	−177.2 (4)	C4—C5—C6—C7	−1.0 (6)
S1—C1—N1—C2	0.7 (3)	C4—C3—C2—C7	−0.5 (5)
N1—C2—C3—C4	178.3 (4)	C3—C2—N1—C1	−178.9 (4)
N1—C2—C7—C6	−178.1 (3)	C3—C2—C7—C6	0.7 (4)
N1—C1—S1—C7	−0.8 (3)	C3—C4—C5—C6	1.2 (6)
N3—C8—S2—C14	−0.5 (3)	C7—C2—N1—C1	−0.1 (4)
N3—C9—C14—C13	178.4 (4)	C10—C9—C14—C13	−0.6 (5)
N3—C9—C10—C11	−179.2 (5)	C10—C11—C12—C13	−2.3 (7)
F1—C5—C4—C3	−178.9 (4)	C1—S1—C7—C6	178.1 (3)

Hydrogen-bond geometry (Å, º)

*Cg*1 and *Cg*6 are the centroids of the Zn1/O1/C15/O2 and S1/N1/C1–C7 rings, respectively.

D—H···*A*	*D*—H	H···*A*	*D*···*A*	*D*—H···*A*
N2—H2B···O4^{i}	0.86 (1)	1.97 (1)	2.806 (5)	162 (1)
N4—H4B···F2^{ii}	0.86 (1)	2.44 (1)	2.910 (6)	115 (1)

N4—H4B···O2^{iii}	0.86 (1)	2.07 (1)	2.890 (4)	160 (1)
C18—H18B···*Cg*6^{iv}	0.96 (2)	2.97 (2)	3.565 (5)	121 (1)
C17—O4···*Cg*1	1.22 (1)	3.08 (1)	3.234 (4)	86 (1)

Symmetry codes: (i) −*x*+1, −*y*+1, *z*+1/2; (ii) *x*+1/2, −*y*+3/2, *z*−1; (iii) *x*+1/2, −*y*+3/2, *z*; (iv) *x*, *y*, *z*−1.